



Rapid phenotypic characterization of *Salmonella enterica* strains by pyrolysis metastable atom bombardment mass spectrometry with multivariate statistical and artificial neural network pattern recognition

Jon G. Wilkes*, Larry Rushing, Rajesh Nayak, Dan A. Buzatu, John B. Sutherland

National Center for Toxicological Research, FDA, 3900 NCTR Drive, Jefferson, AR 72079, United States

Received 28 May 2004; received in revised form 13 December 2004; accepted 14 December 2004

Abstract

Pyrolysis mass spectrometry was investigated for rapid characterization of bacteria. Spectra of *Salmonella* were compared to their serovars, pulsed-field gel electrophoresis (PFGE) patterns, antibiotic resistance profiles, and MIC values. Pyrolysis mass spectra generated via metastable atom bombardment were analyzed by multivariate principal component-discriminant analysis and artificial neural networks (ANNs). Spectral patterns developed by discriminant analysis and tested with Leave-One-Out (LOO) cross-validation distinguished *Salmonella* strains by serovar (97% correct) and by PFGE groups (49%). An ANN model of the same PFGE groups was cross-validated, using the LOO rule, with 92% agreement. Using an ANN, thirty previously unseen spectra were correctly classified by serotype (97%) and at the PFGE level (67%). Attempts by ANN to model spectra grouped by resistance profile-but ignoring PFGE or serotype-failed (10% correct), but ANNs differentiating ten samples of the same serotype/PFGE class were more successful. To assess the information content of PyMS data serendipitously associated with or directly related to resistance character, the ten isolates were grouped into four, three, or two categories. The four categories corresponded to four resistance profiles. The four class and three class ANNs showed much improved but insufficient modeling power. The two-class ANN and a corresponding multivariate model maximized inferential power for a coarse antibiotic-resistance-related distinction. They each cross-validated by LOO at 90%. This is the first direct correlation of pyrolysis metastable atom bombardment mass spectrometry with immunological (e.g. serology) or molecular biology (e.g. PFGE) based techniques.

© 2004 Elsevier B.V. All rights reserved.

Keywords: *Salmonella*; PyMS; MAB; ANN

* Corresponding author. Division of Chemistry, NCTR, Jefferson, AR 72079, United States. Tel.: +1 870 543 7108; fax: +1 870 543 7686.
E-mail address: jwilkes@nctr.fda.gov (J.G. Wilkes).

1. Introduction

Phenotypic methods for rapid bacterial characterization may be useful if they can characterize both target and unanticipated bacteria. One application would be early detection of an outbreak caused by bioterror agents, when there might be little symptomatic, and no contextual or epidemiological, basis for characterizing the agent (Meyer and Morse, 2002; Snyder, 2003). Another is the unsolved public health challenge of antibiotic resistance (Louie and Cockrill, 2001). Resistant strains are increasing in an evolutionary process only partially reversible when the exposure stimulus is removed (Salyers and Amábile-Cuevas, 1997). Survival of resistant bacteria is enhanced by agricultural prophylactic use of antibiotics (Butaye et al., 2003; Salyers, 2002) and physicians' writing of antibiotic prescriptions before knowing the pathogen's susceptibility (Conly, 2002; Louie and Bell, 2002). Both sources of selective pressure could be reduced if there were an available method with general (rather than target) applicability, sensitive detection, that allowed rapid characterization, was robust and cost-effective. Certain analytical instruments, particularly if they do not require time-intensive chromatography, can meet the criteria involving generality, rapidity, and low cost/unit analysis. With such instruments, taxonomic power is the remaining issue.

This work investigates an instrumental/computational system (Dephy Technologies, Montréal, Québec, Canada) for phenotypically characterizing bacterial samples. Its analytical foundation is pyrolysis mass spectrometry (PyMS), using metastable atom bombardment (MAB) with a time-of-flight (ToF) mass analyzer. Sample spectra are classified by computerized pattern recognition. PyMS for bacterial characterization has been studied extensively using electron ionization and a variety of pattern recognition methods. (Cartmill et al., 1992; Freeman et al., 1991; Goodacre and Kell, 1996b; Goodacre et al., 1998; Gould et al., 1991; Low et al., 1992; Orr et al., 1991; Sisson et al., 1991a,b,c, 1992a,b).

Bacterial chemotaxonomy by PyMS was deemed impractical for comparative assays over periods greater than 30 days because the patterns were not sufficiently stable (Goodacre and Kell, 1996a). It was not possible to create and use a database (library) of

standard spectra. In response to this problem, Goodacre and Kell (1996b) published several methods to correct PyMS patterns for distortions from instrumental drift. However, they did not demonstrate the ability to achieve drift correction using a species different from the one by which they characterized the drift, a necessary prerequisite to identify unknown bacteria from a library. In our hands, drift-compensation of "unknown" sample spectra by reference to the drift of other, known species was not consistently successful. The major causes of spectral variation were instrumental drift, as Goodacre and Kell realized, but also sample history. We found that variations in supplier or batch of culture medium caused spectral variations that differed in degree among disparate types of bacteria. This phenomenon was attributed to the differential metabolic capabilities of the bacterial types with respect to changed nutrients.

The dilemma has been resolved. We disclosed a strategy for identifying a microbiological reference strain useful for compensating the spectral drift of an unknown strain (Wilkes et al., 2001). It involves tracking instrumental and cell history variations on the day of analysis. This is done by co-analyzing isolates already in the spectral library, using the variations observed in appropriate reference spectra as an internal standard, a basis for correcting the spectra of unknowns to be identified from the library (Wilkes et al., 2002). The demonstrated feasibility of drift compensation suggests reconsideration of PyMS for rapid, practical chemotaxonomy.

Another issue with PyMS for microbial characterization is the question of its spectral information content. Pyrolysis for chemotaxonomy has been compared to breaking a beautiful vase and attempting to describe it from the shards. By this analogy, mass spectrometric techniques that assay whole proteins, large peptides, or other large biomolecules should give a more representative picture of cell contents (the intact or less damaged vase) and yield a more reliable characterization. Investigators have used fast atom bombardment (Sadek et al., 1998; Radcliffe et al., 2001), electrospray (Johnson et al., 2000), and MALDI ionization (Arnold and Reilly, 1998; Claydon, 2000; Bundy and Fenselau, 2001; Conway et al., 2001; Smole et al., 2002; Leuschner et al., 2003) with mass spectrometric analyzers of varying sophistication (Black and Fox, 1996; Jones et al., 2003). As

expected, these methods have much greater ability than PyMS to detect and identify proteins or other macromolecular biomarkers and to elucidate the relationships among the detected biomarkers and bacterial characteristics. They can address many aspects of fundamental microbiological research (van Baar, 2000). However, for several reasons, none of the alternative methods is as useful for rapid, strain-level fingerprinting. For example, we have found that MALDI MS spectral patterns contain less reliable indicators of biomarker expression level than PyMS. The irreproducibility of MALDI fingerprints agrees broadly with others' observations (Leuschner et al., 2003). In this work, the spectra for the 29 *Salmonella* isolates analyzed by PyMS shared an identical constellation of MALDI peaks. When analyzed by identical methods, MALDI mass spectra could not support strain distinctions (data not shown) apparent in PyMS patterns (reported below).

We have continued to investigate PyMS for rapid screening. The Py-MAB-MS system offers substantial advantages relative to previous PyMS approaches, as does a novel artificial neural network computational platform used here.

In metastable atom bombardment (MAB), ionization processes occur such that spectral drift is minimized. MAB is being developed for mass spectrometric analysis of small molecules (Cyr et al., 1996; Faubert et al., 1993; Bertrand et al., 2000). Ionization occurs by generating metastable species, typically from a noble gas or nitrogen (N_2) plasma, and allowing these to interact, at low kinetic energy, with neutral gas-phase analytes. If the metastable species' internal energy above ground state exceeds that of the analyte's ionization potential (IP), a transfer of energy from metastable to analyte occurs. This causes a return to ground state of the former and ionization of the latter. Since the internal energy states available to metastables are constrained by quantum mechanics, all excess energy must be imparted to the analyte. The magnitude of excess energy imparted to an analyte molecule equals the difference between its IP and the metastable's energy. Metastable ionization leads to a fragmentation pattern characteristic of the bond locations and strengths of the analyte as they relate to the amount of excess energy absorbed. Efficiency of energy transfer is independent of angle of incidence and molecular

orientation, so the resulting fragmentation pattern is essentially independent of instrumental conditions. This quality commends MAB for bacterial characterization, in which spectral reproducibility is a sine qua non.

The amount of energy transferred in MAB is adjusted for each application by using gases in which the available metastable states differ in the amount of energy above their ground state. Interacting with a low energy metastable such as Xe^* , Kr^* , or N_2^* , a typical analyte's molecular fragmentation is minimal. A greater proportion of analyte spectral information is represented in either intact molecular ions or, for the Py-MS experiments here, first generation thermal fragments. For a complex mixture of bacterial cell components, the result is an average Py-MS spectrum containing heavier ions than a corresponding 70 eV (high excess energy) Py-EI-MS spectrum.

For bacterial characterization by MAB, there is an optimal choice between the available energetic extremes of He^* (19.8 eV) and Xe^* (8.3 eV). One selects a metastable species capable of ionizing biomarkers characteristic of cell identity but having too little energy to ionize background components.

Thus, MAB can give high-, medium- or low-energy ionization. In medium- or low-energy mode, it can produce a spectrum blind to some sample components (perhaps impurities). MAB generated ions are either true molecular ions (not protonated molecules) or the same kind of fragments (obeying well-understood fragmentation and rearrangement rules) produced by electron ionization (EI). Generally, MAB gives greater spectral reproducibility than conventional 70 eV EI (Mousselmal et al., 1996; Mireault et al., 1996). Together, these capabilities commend Py-MAB-MS for the analysis of biological samples, sometimes with minimal preparation (Dumas et al., 2002).

Two methods used for pattern recognition are principal component-discriminant analysis (Shen et al., 2003) and error-backpropagating artificial neural networks (ANNs) (Rumelhart and McClelland, 1986). For principal component-discriminant analysis, a qualitative interpretation of results is possible using score-plots. Clustering and spatial relationships of sample identifier symbols appearing on 2-D score-plots are used here to investigate the characterization capabilities of the Py-MAB-MS system.

ANNs are mathematical models with connection geometry analogous to neurons in the brain. By trial and error using different combinations of weights for the connections, they are “trained” to recognize complex relationships among input and output data elements. The input data might be a group of mass spectra and the output, bacterial strains associated with each spectral pattern. Once an ANN has been trained and validated, one can enter new spectra and associate each spectrum with similar output categories. In comparison to principal component-discriminant analysis, ANNs have been found more reliable for predicting category membership when relationships among input and output are complex or non-linear (Spining et al., 1994).

ANN architecture development is traditionally done by manual setup of each configuration with iterative attempts to find the best one. It involves assembly-line setup and serial computation, which is inefficient. We wrote a parallel-distributed artificial neural network (PD-ANN) program that uses a team of ethernet-connected personal computers to automate survey and validation of ANN feature-space. This allowed identification of global optimum configurations for each ANN. Therefore, objective comparisons were possible between ANN and discriminant analysis.

To examine chemotaxonomic power of the combined Py-MAB-MS and computational system, we used a test set of *S. enterica* isolates found in a single ecosystem. These strains represented the range of diversity in a real-world environment rather than an arbitrary selection from a culture collection in which great sample diversity would tend to assure the likely success of the differentiation effort. The isolates studied here, while highly similar in most ways, exhibited subtle differences in immunological, genetic, and antibiotic-resistance characteristics. Distinguishing the test set isolates posed a substantial challenge to the system. This task was relevant to diagnostic needs summarized above, complex enough to illumine bases for class distinctions, and rigorous enough to establish a performance baseline.

This sample set comprised species that impact food safety and have been used for bioterrorism/biowarfare (Török et al., 1997; B. Gellman, March 23, 2003, The Washington Post, Page A1). The first citation describes a well known past instance of food-borne

bioterrorism and the second, a *Salmonella* sp. militarized by al Qaeda for use against U.S. soldiers in Afghanistan. Widespread clinical availability of rapid microbial characterization could accelerate recognition of a biological agent attack. Rapid strain distinction would have forensic significance and might enable informed drug prescription, thus helping to slow proliferation of antibiotic-resistant strains.

This is the first direct correlation of pyrolysis metastable atom bombardment mass spectrometry with immunological (e.g. serology) or molecular biology (e.g. PFGE) based techniques.

2. Materials and methods

2.1. Bacterial cultures

Samples were collected from one turkey production facility. Strains were isolated from drinkers, turkey caeca, feeder contents, litter or surface swabs (Nayak et al., 2004). Isolates were characterized with respect to their antibiotic-resistance profile using the disk diffusion assay (NCCLS, 1993) and further tested for their minimum inhibitory concentration (MIC) values by the macro-broth dilution assay (NCCLS, 1998). *S. enterica* ser. Typhimurium ATCC 14028 was used for comparison.

2.2. Restriction analysis of chromosomal DNA

The method used is specified for *Salmonella* by the US Centers for Disease Control and Prevention. Bacterial colonies were suspended in 1–2 ml of cell suspension buffer (100 mM Tris-HCl and 100 mM EDTA, pH 8.0). The optical density (610 nm) of the cell suspension was standardized to 1.3–1.4 mg/l. An aliquot (400 μ l) of cell suspension was mixed with 20 μ l of proteinase K (20 mg/ml) and 400 μ l of 1% SeaKem Gold agarose (BioWhittaker Molecular Applications, Rockland, ME, USA) and 1% SDS prepared in TE buffer (10 mM Tris-HCl and 1 mM EDTA, pH 8.0). The bacterium-agarose mixture was dispensed into plug molds and allowed to solidify at room temperature for 10–15 min. Each sample plug was transferred to a 50 ml Nalgene centrifuge tube containing 5 ml cell lysis buffer (50 mM Tris-HCl and 50 mM EDTA, pH 8.0+1% sodium N-lauroyl-

sarcosinate). Proteinase K was added to each tube to give a final concentration of 0.1 mg/ml. The tubes were incubated in a water bath maintained at 54 °C for 2 h with constant agitation (175–200 rpm). After proteolysis, plugs in each tube were washed once with 10–15 ml of preheated (50 °C) distilled water and four times with preheated (50 °C) sterile TE buffer for 10–15 min each time. Each sample plug was digested with 50 units of *Xba*I (Invitrogen, Carlsbad, CA, USA) at 37 °C for 5 h. The DNA bands were separated on 1% SeaKem Gold agarose by the CHEF-Mapper III pulsed field gel electrophoresis (PFGE) system (Bio-Rad Laboratories, Hercules, CA, USA) using the following electrophoretic conditions: initial switch time, 2.16 s; final switch time, 63.8 s; run time, 18 h; angle, 120°; gradient, 6.0 V/cm; temperature, 14 °C; ramping factor, linear. After electrophoresis, gels were stained with ethidium bromide and images were captured with a gel documentation system.

2.3. Statistical analysis of PFGE patterns

The genetic relationships among the *Salmonella* strains were analyzed using Bionumerics software (Applied Maths, Kortrijk, Belgium). PFGE patterns were deemed equivalent when the banding patterns shared >95% genetic homology. The similarity matrix and dendrogram type used for cluster analyses were calculated by the “Dice” band matching coefficient and the “Unweighted Pair Group Method using Arithmetic Mean (UPGMA)” algorithm, respectively. A positional tolerance shift of 1% of pattern length was allowed between similar bands and an optimization shift of 0.5%, between any two patterns.

2.4. Cell preparation for PyMS

Each strain was incubated in trypticase soy broth for 3 h at 37 °C with shaking at 250 rpm. Cell suspensions were centrifuged at 6572 ×g for 7 min; supernatant was discarded. Pellets were washed with 800 µL of phosphate-buffered saline (Gibco BRL Life Technologies, Gaithersburg, MD), centrifuged, decanted, and resuspended in saline. After another centrifugation/decanting step, the cells were suspended in 200 µL of ethanol:water (70:30, v/v). Suspensions were stored at –70 °C before PyMS analysis.

2.5. Pyrolysis method

Before each analysis, suspensions were thawed and resuspended by mixing for a few seconds with a Daigger Vortex Genie 2 (Scientific Industries, Bohemia, NY). A small aliquot was taken up with a GC sample injection syringe and 0.2–0.5 µL (5.0–7.5 × 10⁴ cells) was dispensed onto the rhenium wire loop of a Direct Exposure Probe (DEP, Finnigan Corporation, Sunnyvale, CA). After solvent evaporation, the DEP was inserted through the vacuum lock directly into the MS ion source. MS data acquisition and pyrolysis were initiated simultaneously. The pyrolysis program was a linear ramp from 100 to 600 mA at 20 mA/sec. Each mA corresponded to ~1.0 °C.

2.6. Instrumental details

The PyMS instrument was a MAB-Tof (Dephy Technologies, Montréal, Québec, Canada) with a 2000 amu range. The mass spectrometer ion source body was operated at a relatively low 150 °C to minimize thermal fragmentation of labile biomolecules. Over a mass range of *m/z* 60–599, ~19,000 full scan spectra were sampled and combined to produce an average spectrum every 0.2 s. Data were acquired in peak-area detection mode.

Ionization employed Ar* (11.5 or 11.7 eV) as the metastable species. Argon MAB gas pressure was 50 mBar; discharge current was 9.5 mA at 420 V.

2.7. Data acquisition

The MAB/Tof MS has three detectors with different sensitivities. Experimental variables were adjusted so ions would not saturate the most sensitive detector, TDC1. With such small samples, only a few ions were consistently detectable above *m/z* 250. Spectral range used was reduced from that acquired (*m/z* 60–599) to *m/z* 60–250 for discriminant analysis and *m/z* 60–252 for ANN pattern recognition. Background ions at *m/z* 70, 72, and 80 were deleted.

The *Salmonella* suspensions were analyzed using improved procedures. After preliminary optimization we: (a) switched MAB gas from krypton (9.9 eV) to argon (11.5 eV); (b) detected MS peak-

area rather than peak-top; (c) reduced sample sizes as described above; and (d) averaged the entire pyrogram peak rather than the top half only. Choice (a) was for economy. Choice (b) was to avoid having multiple peaks for the same nominal mass when the signal intensity was low. Item (c) avoided electronic anomalies associated with detector switch-over in the Tof MS electronics and the ~20-fold worse signal-to-noise produced by the less sensitive detectors. In (d), we began averaging over the whole pyrolysis peak to include reproducibly contributions of high and low volatility pyrolysates.

Spectra were exported to RESolve version 1.1 (Colorado School of Mines, Golden, CO) for principal component-discriminant analysis and, for ANN modeling, to the previously described parallel distribution facility developed at the National Center for Toxicological Research.

2.8. Principal component-discriminant analysis

Principles of this type analysis have been described elsewhere (Beebe et al., 1998) except for the use of a category-reduction strategy comparing, in successive assays, fewer possible identities for each unknown. The analyst chooses approximately 15 principal components of variation (PCs) and builds a discriminant function model for N spectra grouped into M classes. Normally the model is tested by leave-one-out (LOO) cross-validation. In LOO, each spectrum is temporarily excluded from the test set, the model is rebuilt, and the new model is used to classify the excluded spectrum. To improve results, models can be built using a different number of PCs and compared by LOO. By examining plot distances between an unknown and known samples, one can eliminate consideration of dissimilar, distant categories. One constructs new comparison sets (RESolve files) that include only those categories closest to each unknown. Since in the smaller sets the discriminant functions are calculated to distinguish fewer categories, the model shows improved classification. Clusters are better separated, and LOO cross-validation results improve. The category-reduction strategy is particularly useful when the sample set comprises many similar but significantly different strains.

2.9. ANN analysis

The process used a team of ethernet-connected personal computers with a parallel distributed (PD) program. During architecture optimization, the quality of each ANN model was assessed by cross-validation. 100 spectra (at least triplicates for each of the *S. enterica* strains) were acquired. Five types of ANN analysis were performed.

First, the data set was divided into a training set of 70 and test set of 30 spectra classified into 12 groups, based on PFGE similarity (see PFGE results below). To determine the optimal number of hidden layer nodes, the PD-ANN systematically surveyed all values between $N/3$ and $2N+1$, where $N=190$, the number of nodes in the input layer. Each test architecture proceeded for 20,000 feed-forward-back-propagation iterations (learning cycles), after which its predictions on the 30 test set spectra were compared to the other architectures. After optimization of this fully connected, three layer ANN (Rumelhart and McClelland, 1986), the optimal model was identified as having 190-63-12 architecture and sigmoidal transfer functions.

Second, using the optimal architecture and the same 12 groups, we built 100 models trained on 99 spectra and tested each for predictive accuracy on the one excluded (LOO). We also built a single model using all 100 spectra and compared its accuracy to accuracy for combined results from the 100 LOO models.

A third ANN model used a 30 spectra subset of 10 Heidelberg strains with the same PFGE-assayed genetics but four different antibiotic-resistance profiles, each represented by one of the output layer nodes in a 190-63-4 architecture.

Using the same ten strains as the third ANN, two more resistance models were developed having 190-63-3 and 190-63-2 architecture, respectively. The rationale for these models will be discussed following results of the antibiotic resistance and PFGE analyses.

3. Results

3.1. Antibiotic resistance and PFGE

Of 29 isolates from the turkey production facility, all were *Salmonella enterica* serovar Anatum,

Heidelberg, Worthington, or Muenster (Table 1). All were resistant to erythromycin, bacitracin, novobiocin, and rifampin. Some isolates of the same serovar differed in antibiotic-resistance profile. Many with the same antibiotic-resistance phenotype differed in resistance strength.

The four antibiotics to which all isolates were resistant differed from each other in their therapeutic mechanism (Willett, 1988). Erythromycin binds to the 50 S ribosomal subunit and prevents protein synthesis. Bacitracin interferes with peptidoglycan biosynthesis in the cell wall. Novobiocin inhibits DNA gyrase. Rifampin inactivates RNA polymerase. Thus, every strain harvested from the turkey production facility exhibited antibiotic resistance by at least four mech-

anisms. Also, 22 of 29 were resistant to at least one other of ten antibiotics commonly used in the poultry industry or for treatment of salmonellosis. Streptomycin, gentamicin, tetracycline, and spectinomycin bind to the 30 S ribosomal subunit and prevent protein synthesis. Sulfamethoxazole and trimethoprim inhibit tetrahydrofolate synthesis (Willett, 1988). Together, the turkey farm isolates exhibited resistance to antibiotics operating by six mechanisms. This test set exemplified the public health significance of antibiotic resistance proliferation.

PFGE patterns were arrayed by similarity using a dendrogram (Fig. 1). Patterns with genetic homology >95% were deemed equivalent. PFGE clearly segregated samples into the four serovars. The four

Table 1

Salmonella enterica isolates from a turkey farm, each characterized by serovar, antibiotic-resistance phenotype, and MIC values. Symbols used in Figs. 2–4 are also shown

ID no.	Symbols	Serovar	Antibiotic-resistance phenotype*	MIC (µg/mL)						
				Te	St	Ge	Spt	Er	Ri	No
1	△	Anatum	Te St Er B No Ri	512	256	>256		128	512	>1024
2	▲	Anatum	Te St Er B No Ri	256	256	>256		128	512	>1024
3	△	Anatum	Te St Er B No Ri	256	256	>256		256	256	>1024
4	a	Heidelberg	Er B No Ri					512	128	>1024
5	b	Heidelberg	Te Sxt Er B No Ri	128				128	256	>1024
6	c	Heidelberg	St Spt Ge Er B No Ri		>256	256	>512	>512	512	>1024
7	d	Heidelberg	St Spt Ge Er B No Ri		>256	256	>512	128	1024	>1024
8	e	Heidelberg	Er B No Ri					512	512	>1024
9	f	Heidelberg	St Spt Ge Er B No Ri		>256	256	>512	512	1024	>1024
10	g	Heidelberg	Te St Spt Ge Er B No Ri	256	>256	>256	>512	512	1024	>1024
11	h	Heidelberg	St Spt Ge Er B No Ri		>256	256	>512	512	1024	>1024
12	j	Heidelberg	Er B No Ri					256	1024	>1024
13	k	Heidelberg	St Spt Ge Er B No Ri		>256	256	>512	512	1024	>1024
14	l	Heidelberg	St Spt Ge Er B No Ri		>256	256	>512	512	1024	>1024
15	m	Heidelberg	St Spt Ge Er B No Ri		>256	>256	>512	512	512	>1024
16	n	Heidelberg	St Spt Ge Er B No Ri		>256	256	>512	256	512	>1024
17	●	Worthington	Te Er B No Ri	32				128	512	>1024
18	p	Heidelberg	St Spt Ge Er B No Ri		>256	256	>512	128	1024	>1024
19	q	Heidelberg	Er B No Ri					256	1024	>1024
20	r	Heidelberg	St Spt Ge Er B No Ri		>256	256	>512	512	512	>1024
21	r	Heidelberg	St Spt Ge Er B No Ri		>256	>256	>512	128	512	>1024
22	r	Heidelberg	St Spt Ge Er B No Ri		>256	256	>512	128	1024	>1024
23	s	Heidelberg	Er B No Ri					256	1024	>1024
24	u	Heidelberg	Te St Spt Ge Er B No Ri	256	>256	128	>512	256	1024	>1024
25	v	Heidelberg	Er B No Ri					256	512	>1024
26	●	Worthington	Te Er B No Ri	32				64	1024	>1024
27	●	Worthington	Te Er B No Ri	32				128	1024	>1024
28	□	Muenster	Er B No Ri					512	1024	>1024
29	■	Muenster	St Ge To Te Er B No Ri		>256	>256		32	1024	>1024

* Te, Tetracycline; St, Streptomycin; Ge, Gentamicin; Spt, Spectinomycin; Sxt, Sulfamethoxazole:trimethoprim cocktail; Er, Erythromycin; To, Tobramycin; Ri, Rifampin; No, Novobiocin; B, Bacitracin.

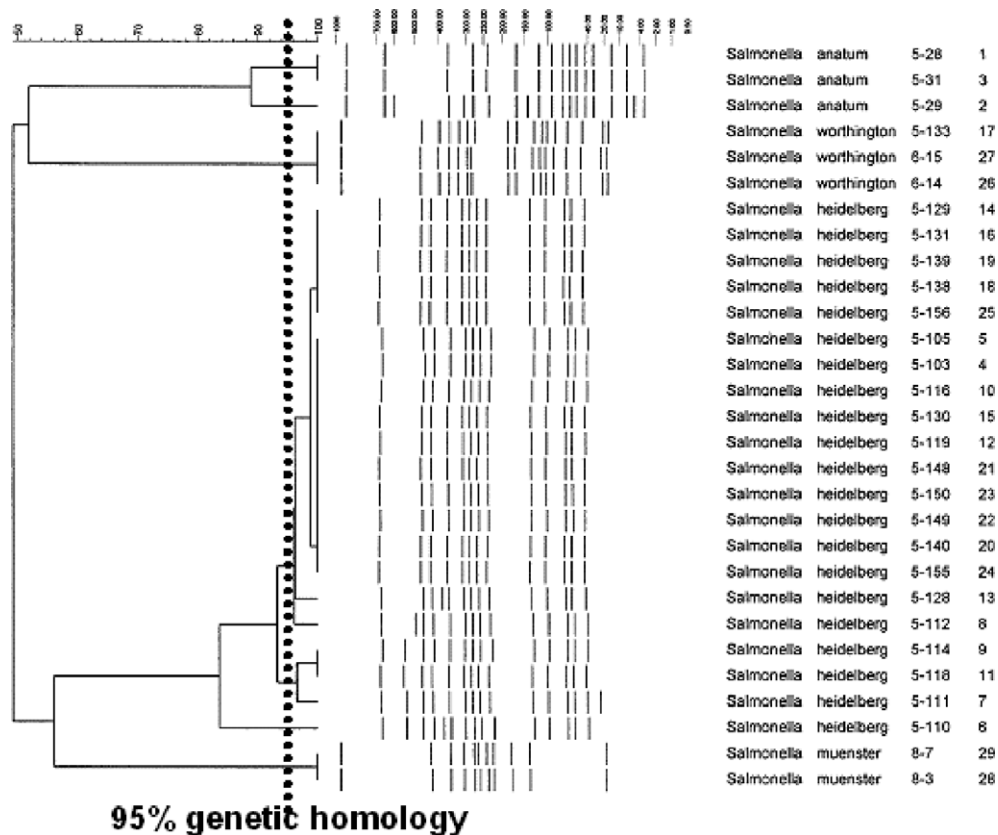


Fig. 1. PFGE patterns and dendrogram for the 29 isolates of *S. enterica*. A *S. enterica* serovar Typhimurium control not shown in this figure was also analyzed by Py-MAB-MS.

serovars differed in antibiotic-resistance phenotype from each other (Table 1). The two Muenster isolates, 28 and 29 (identical by PFGE, Fig. 1) differed in antibiotic-resistance phenotype (Table 1). The three Worthington isolates (identical by PFGE and antibiotic-resistance phenotype) differed somewhat in MIC values (Table 1). Note that strains appearing identical in every column of Table 1 could differ in non-assayed characteristics. Of the three Anatum PFGE profiles, sample 2 had four extra PFGE bands, different from the others (Fig. 1). However, the three shared the same antibiotic-resistance phenotype and differed only slightly in MIC values, implying that the four bands were not resistance-associated.

By PFGE, one Heidelberg (sample 6) appeared to differ strongly from the other Heidebergs, sharing only 84% genetic homology with them. Three other

Heidebergs (samples 7, 9, and 11) also differed significantly from the majority of that serovar. Table 1 does not show any obvious correlation between PFGE distinction and antibiotic-resistance phenotypes or MIC values of these four Heidelberg outliers. This is not surprising since resistance in bacteria is typically associated with plasmids. So, even though the four serovars differed in antibiotic-resistance phenotype, those differences did not explain PFGE distinctions.

3.2. Resistance profile and ANN design

Heidebergs 4, 5, 10, 12, 15, and 20–24 were equivalent by PFGE but had four different antibiotic resistance phenotypes. An ANN model with architecture 190-63-4 was built based on these four. After evaluating systematic errors in this model, another

was developed with only three classes: architecture 190-63-3. Finally, a 190-63-2 ANN was built with only two classes, “A” and “B”. Class “A” consisted of strains 12 and 23 with the minimal resistance profile: (resistance to erythromycin, bacitracin, novobiocin, and rifampin). Group “B” contained strains 4, 5, 10, 15, 20, 22, and 24, all but one of which possessed additional resistance.

3.3. Py-MAB-MS using principal component-discriminant analysis

Spectra were used without centroiding or weighting. Data pre-processing included: (1) deleting background ions (2) deleting all ions from m/z 250–599 where few peaks were observed; (3) class categorizing using an alpha-numeric character; and (4) normalizing all spectra with respect to total ion intensity. The pyrolysis argon MAB spectra so edited included signal at each mass, so distinctions depended on

consistent interclass differences in relative ion intensity rather than unique biomarkers. Figs. 2, 3, and 4 are discriminant function (canonical variate) score-plots, based on the Py-MAB-MS spectra. Viewed in sequence, they show results from systematically reducing the number of possible identities for an ‘unknown’, indicated by the symbol “0”. The unknown was Heidelberg 13 (symbol “d”).

Fig. 2 is the discriminant function score-plot, Component 1 vs. Component 2, using 15 PCs. For three of the four serovars, geometric symbols signify one or more strains: “ Δ ” or “ \blacktriangle ” for Anatum, “ \square ” or “ \blacksquare ” for Muenster, and “ \bullet ” for all three Worthingtons. Heidelberg strains were labeled using lower case letters. Heidelberg strains were labeled using lower case letters. Non-replicates were assigned the same alphanumeric symbol if their PFGE and antibiotic-resistance phenotypes were equivalent. The unknown appears, correctly, among the cluster of letters representing the Heidelberg. Heidelberg 6s (symbol c), the most prominent outlier by PFGE, appear in

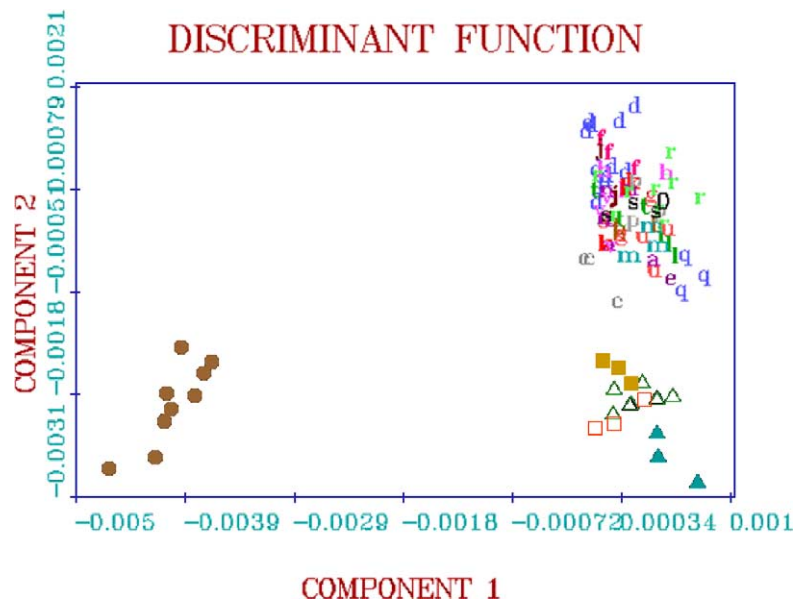


Fig. 2. Discriminant function score-plot of Component 1 vs. Component 2, based on 15 PCs. For three of the four turkey farm serovars, geometric symbols signify one or more strains: “ Δ ” or “ \blacktriangle ” for Anatum, “ \square ” or “ \blacksquare ” for Muenster, and “ \bullet ” for all three Worthingtons. The strains of serovar Heidelberg, comprising the great majority of those studied, were labeled using lower case letters as was the serovar Typhimurium control (symbol t). The sample marked 0 is a Heidelberg strain assigned unknown status to evaluate here (and in Figs. 3 and 4) the utility of the category-reduction process. Samples 6, 7, 9, and 11 (symbols c, d, f, and g)—classified by PFGE as outliers compared to the other Heidelberg—appear on the edges of the cluster of Heidelberg letters in this plot. Heidelberg strain 6, the most dissimilar by PFGE, also appears in this PyMS-based score plot as c, most detached from the Heidelberg cluster. Together these observations indicate that features in PyMS correspond qualitatively to serotype and also to patterns in PFGE patterns.

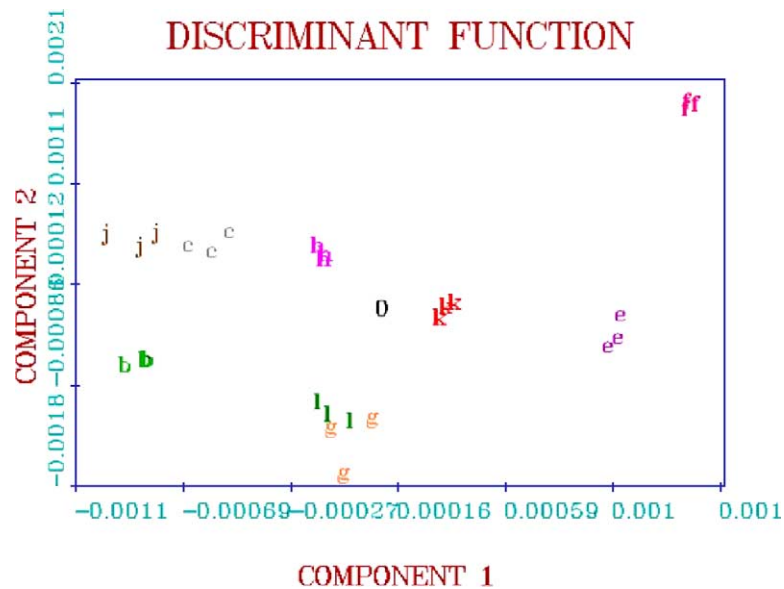


Fig. 3. Discriminant function score-plot of Component 1 vs. Component 2, based on 15 PCs, of nine Heidelberg isolates grouped by their PFGE and antibiotic-resistance phenotypes. The **0** appears near Heidelberg symbols **h**, **k**, and **l**, which correspond to sample I.D. numbers 11, 13, and 14, respectively.

Fig. 2 as the most prominent outlier at the edge of the Heidelberg cluster. A similar relationship holds for samples 7 (symbol **d**), 9 (symbol **f**), and 11

(symbol **h**). All four Heidelberg outliers observed in the PFGE-based dendrogram were outliers in this plot based on Py-MAB-MS spectra.

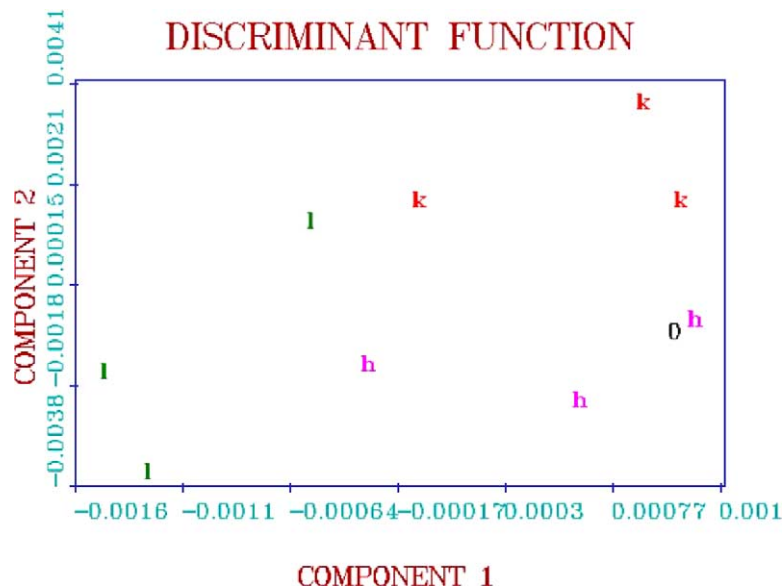


Fig. 4. Discriminant function scoreplot of Component 1 vs. Component 2, based on 5 PCs, showing only the unknown **0** and the three most similar of the Heidelberg isolates. The unknown appears grouped with either sample **h** or **k**. Isolate 13 represented by **k** is correct and strain 11 shown as **h** is almost right, since both are identical in serotype, antibiotic resistance phenotype, and MIC values while sharing 94% genetic similarity by PFGE.

In the first step of category reduction, all non-Heidelberg serovars were omitted. The remaining categories and the unknown were re-analyzed, again using 15 PCs. This process was repeated, removing one or two outliers at a time. Fig. 3 is a score-plot obtained part way through. The unknown appears, correctly, near the cluster of letters **k**, the symbol chosen to represent strain 13. Fig. 4 shows a score-plot based on 5 PCs, when only **h**, **k**, and **l** remained. The unknown appears grouped with either sample **h** or **k**. The isolate represented by **k** is correct and strain **h** is very similar to it, since both are identical in serotype, antibiotic resistance phenotype, and MIC values.

Comparison of Fig. 2 with Fig. 1 and Table 1 shows that Py-MAB-MS characterization of the isolates having non-Heidelberg serovars was consistent with differences in serovar, PFGE pattern, and antibiotic resistance. The two Muenster strains, identical by PFGE but different in antibiotic-resistance phenotype, show in Fig. 1 as two distinct clusters, “■” and “□”. In this RESolve file, three spectra of a *Salmonella enterica* ser. Typhimurium ATCC 14028 (not in Table 1; symbol **t**) were included. The **t**'s overlap the Heidelberg symbols here but were separated when viewed in the Component 3 vs. Component 4 plane (data not shown).

Separate analysis of Worthingtons showed significant and consistent differences among their spectra (data not shown). On a 2-D score-plot based on the first two PCs, the three clusters were well separated. These spectral differences presumably were based on factors not measurable by PFGE and not represented in the antibiotic-resistance phenotype. The MIC values for the three Worthington isolates were not identical, and this might constitute the biological basis for their distinction by Py-MAB-MS. Worthington and Muenster results suggested that Py-MAB-MS may differentiate strains on the basis of resistance.

Using the original data acquisition parameters from preliminary experiments, the three Worthington strains could not be distinguished (data not shown). Results in this work, therefore, demonstrate significant improvement in power to differentiate similar but non-identical strains, a consequence of the greater spectral reproducibility from the improved procedures.

3.4. Py-MAB-MS using the parallel distributed ANN, modeling based on serology and PFGE patterns

The ANN architecture had an input layer of 190 nodes, one for each ion. The optimal hidden layer contained 63 nodes. The output layers varied depending on categorization task. For example, the first two models contained 12 nodes, one for each *S. enterica* category distinguished by PFGE plus one more to represent the aforementioned Typhimurium control. Using the 190-63-12 optimal architecture, iterations ranging from 10,000 to 100,000 were tested and 40,000–60,000 represented optimal training. This architecture with 40,000 iterations was used to build the single model of 100 spectra as well as the 100 models of 99 spectra for LOO. ANN quantitative accuracy on the single 100-spectra model had a coefficient of regression, $r^2=0.97$. This represents 97 of the 100 spectra correctly classified by PFGE pattern. For values tabulated from the 100 LOO cross validation experiments, an excellent average cross-validation covariance coefficient, $q^2=0.92$, was obtained. That is, 92% of the spectra were correctly classified even when they made no contribution to the model by which they were categorized. This is an excellent result when compared to only 49% by the best corresponding discriminant model.

Using the 190-63-12 architecture and 60,000 iterations, the ANN was also trained on 70 of the spectra and asked to predict 30 test spectra (a Leave-30-Out cross-validation). It was able to classify correctly 20 of the 30 spectra (67%). When broken down by strain, the correct predictions were 2 of 3 Anatumis (67%), 3 of 3 Worthingtons (100%), 2 of 2 Muensters (100%), 1 of 1 Typhimurium (100%), and 12 of 21 combined Heidelbergs (57%). All of the missed Heidelberg classifications involved confusion among other Heidelberg strains. Therefore, when classifying 30 previously unseen spectra by serovar, the optimized ANN trained on 70 spectra was 97% correct.

3.5. Py-MAB-MS using the parallel distributed ANN with modeling based on antibiotic resistance patterns

Attempts by ANN to model all 100 spectra when they were grouped into 12 antibiotic resist-

ance profile categories (i.e. ignoring PFGE or serotype) gave very poor results ($Q_{30}^2=0.10$), only that expected for random guesses among 12 classes. This suggested that PFGE and serotype characteristics are reflected in more prominent biomarkers than is resistance. The poor results do not prove that PyMS spectra are altogether missing resistance-associated information. Indeed, results for the other serovars suggested existence of spectral information directly or co-incidentally associated with resistance.

To access this information for Heidelberg, we tried three designs that eliminated irrelevant contributors to spectral variation using 4, 3, or 2 classes. After satisfactory results were obtained with the 190-63-2 ANN, a corresponding RESolve file was developed for the two classes. Both separated the 10 strains with LOO cross-validation of 90%: for the 190-63-2 ANN, after 15,000 iterations; for RESolve, using eight PCs.

4. Discussion

An important use of the test set was to determine the accessible information content in Py-MAB-MS spectra. Availability of the information depended on the kind of pattern recognition used and diversity of samples compared.

The PyMS and pattern recognition systems demonstrated ability to distinguish strains that differed in serotype, PFGE pattern, antibiotic-resistance phenotype, and in other unidentified factors. The capacity of Py-MAB-MS to distinguish strains based on antibiotic resistance was suggested for Worthington and Muenster strains and was useful for Heidelberg if confounding bases for class identification such as PFGE class were excluded from comparison.

Access via parallel-distribution to a method of determining optimal, rather than merely adequate, ANN architecture allowed objective assessment of Py-MAB-MS's inherent information content. It facilitated modeling experiments to determine which isolates should be regarded as functional equivalents under Py-MAB-MS.

The ANNs performed well, given the difficulty of distinguishing such similar strains. One was able to achieve rapid serotyping with high accuracy. Another

achieved 92% for assessing PFGE profile similarity in a LOO experiment. These are valuable results apart from all other criteria.

We improved resistance classification by removing confounding variables: building ANNs for Heidelberg having the same PFGE pattern but different antibiotic resistance profiles. For coarse antibiotic resistance-based distinction, an ANN and corresponding multilinear model were developed with only two classes, "A" and "B". Applied to unknown characterization, an "A" match would indicate that streptomycin, spectinomycin, gentamicin, tetracycline, or sulfamethoxazole:trimethoprim cocktail could be used for effective therapy. A "B" match would suggest the need to use another antibiotic, for which resistance is presently rare among *Salmonella*. LOO values of 90% correct, whether multilinear or ANN, advocate Py-MAB-MS potential for assaying resistance.

This work demonstrated reliable serotyping and strong classification that paralleled PFGE patterns. Results from three *Salmonella* serotypes suggested that Py-MAB-MS can distinguish samples having dissimilar antibiotic-resistance profiles. We commend Py-MAB-MS for consideration by professionals assessing the diagnostic and forensic needs of clinical, military, and public health laboratories.

Acknowledgement and disclaimer

The authors thank Drs. Fatemeh Rafii and Ashraf Khan for their kind assistance. This work was supported by the National Center for Toxicological Research, US Food and Drug Administration. Views presented here do not necessarily reflect those of the FDA.

References

- Arnold, R.J., Reilly, J.P., 1998. Fingerprint matching of *E. coli* strains with matrix-assisted laser desorption/ionization time-of-flight mass spectrometry of whole cells using a modified correlation approach. *Rapid Commun. Mass Spectrom.* 12, 630–636.
- Beebe, K.R., Pell, R.J., SeaSholtz, M.B., 1998. Pattern recognition. *Chemometrics: A Practical Guide*. Wiley-Interscience, New York, pp. 56–182. Chap. 4.

- Bertrand, M.J., Martin, P., Peraldi, O., 2000. A New Concept in Benchtop Mass Spectrometer, MAB-Tof. PittCon, New Orleans, LA, p. 452. Abstract.
- Black, G., Fox, A., 1996. Liquid chromatography with electrospray ionization tandem mass spectrometry: Profiling carbohydrates in whole bacterial cell hydrolysates. In: Snyder, P. (Ed.), Bio-Chemical and Biotechnological Applications of Electrospray Ionization Mass Spectrometry. American Chemical Society, Washington, DC, pp. 81–105.
- Bundy, J.L., Fenselau, C., 2001. Lectin and carbohydrate affinity capture surfaces for mass spectrometric analysis of microorganisms. *Anal. Chem.* 73, 751–757.
- Butaye, P., Devriese, L.A., Haesebrouck, F., 2003. Antimicrobial growth promoters used in animal feed: effects of less well-known antibiotics on Gram-positive bacteria. *Clin. Microbiol. Rev.* 16, 175–188.
- Cartmill, T.D., Orr, K., Freeman, R., Sisson, P.R., Lightfoot, N.F., 1992. Nosocomial infection with *Clostridium difficile* investigated by pyrolysis mass spectrometry. *J. Med. Microbiol.* 37, 352–356.
- Claydon, M.A., 2000. MALDI-ToF-MS, a new and novel technique for studies of intact cells. *Anaerobe* 6, 133–134.
- Conly, J.M., 2002. Antimicrobial resistance in Canada. *Can. Med. Assoc. J.* 167, 885–891.
- Conway, G.C., Smole, S.C., Sarracino, D.A., Arbeit, R.D., Leopold, P.E., 2001. Phyloproteomics: Species identification of Enterobacteriaceae using matrix-assisted laser desorption/ionization time-of-flight mass spectrometry. *J. Mol. Microbiol. Biotechnol.* 3, 103–112.
- Cyr, M., Faubert, D., Mousselmal, M., Bertrand, M.J., 1996. Analysis of the Emanations from Heated Polyurethane Foam Using MAB-MS. Proc. 44th ASMS Conf. Mass Spectrom. Allied Topics. American Society for Mass Spectrometry, Santa Fe, New Mexico, USA, p. 1267. Portland, OR.
- Dumas, M.-E., Debrauwer, L., Beyet, L., Lesage, D., André, F., Paris, A., Tabet, J.-C., 2002. Analyzing the physiological signature of anabolic steroids in cattle urine using pyrolysis/metastable atom bombardment mass spectrometry and pattern recognition. *Anal. Chem.* 74, 5393–5404.
- Faubert, D., Paul, G.J.C., Giroux, J., Bertrand, M.J., 1993. Selective fragmentation and ionization of organic compounds using an energy-tunable rare-gas metastable beam source. *Int. J. Mass Spectrom. Ion Process.* 124, 69–77.
- Freeman, R., Gould, F.K., Wilkinson, R., Ward, A.C., Lightfoot, N.F., Sisson, P.R., 1991. Rapid inter-strain comparison by pyrolysis mass spectrometry of coagulase-negative staphylococci from persistent CAPD peritonitis. *Epidemiol. Infect.* 106, 239–246.
- Goodacre, R., Kell, D.B., 1996a. Pyrolysis mass spectrometry and its applications in biotechnology. *Curr. Opin. Biotechnol.* 7, 20–28.
- Goodacre, R., Kell, D., 1996b. Correction of mass spectral drift using artificial neural networks. *Anal. Chem.* 68, 271–280.
- Goodacre, R., Timmons, E.A., Burton, R., Kaderbhai, N., Woodward, A.M., Kell, D.B., Rooney, P.J., 1998. Rapid identification of urinary tract infection bacteria using hyperspectral whole-organism fingerprinting and artificial neural networks. *Microbiology* 144, 1157–1170.
- Gould, F.K., Freeman, R., Sisson, P.R., Cookson, B.D., Lightfoot, N.F., 1991. Inter-strain comparison by pyrolysis mass spectrometry in the investigation of *Staphylococcus aureus* nosocomial infection. *J. Hosp. Infect.* 19, 41–48.
- Johnson, Y.A., Nagpal, M., Krahmer, M.T., Fox, K.F., Fox, A., 2000. Precise molecular weight determination of PCR products of the rRNA intergenic spacer region using electrospray quadrupole mass spectrometry for differentiation of *B. subtilis* and *B. atrophaeus*, closely related species of bacilli. *J. Microbiol. Methods* 40, 241–254.
- Jones, J.J., Stump, M.J., Fleming, R.C., Lay, J.O., Wilkins, C.L., 2003. Investigation of MALDI-TOF and FT-MS techniques for analysis of *Escherichia coli* whole cells. *Anal. Chem.* 75, 1340–1347.
- Leuschner, R.G.K., Beresford-Jones, N., Robinson, C., 2003. Difference and consensus of whole cell *Salmonella enterica* subsp. *enterica* serovars matrix-assisted laser desorption/ionization time-of-flight mass spectrometry spectra. *Lett. Appl. Microbiol.* 38, 24–31.
- Louie, J.P., Bell, L.M., 2002. Appropriate use of antibiotics for common infections in an era of increasing resistance. *Emerg. Med. Clin. North Am.* 20, 69–91.
- Louie, M., Cockerill, F.R., 2001. Susceptibility testing: phenotypic and genotypic tests for bacteria and mycobacteria. *Infect. Dis. Clin. North Am.* 15, 1205–1226.
- Low, J.C., Chalmers, R.M., Donachie, W., Freeman, R., McLaughlin, J., Sisson, P.R., 1992. Pyrolysis mass spectrometry of *Listeria monocytogenes* isolates from sheep. *Res. Vet. Sci.* 53, 64–67.
- Meyer, R.F., Morse, S.A., 2002. Bioterrorism preparedness for the public health and medical communities. *Mayo Clin. Proc.* 77, 619–621.
- Mireault, P., Faubert, D., Carrier, A., Mousselmal, M., Bertrand, M.J., 1996. Evaluation of MAB as a Selective Ion Source for Chromatography/mass Spectrometry Technique. Proc. 44th ASMS Conf. Mass Spectrom. Allied Topics. vol. 44. American Society for Mass Spectrometry, Santa Fe, New Mexico, USA, p. 176. Portland, OR.
- Mousselmal, M., Faubert, D., Evans, M.J., Bertrand, M.J., 1996. Comparison of EI and MAB ionization for exact mass measurement. Proc. 44th ASMS Conf. Mass Spectrom. Allied Topics. vol. 44. American Society for Mass Spectrometry, Santa Fe, New Mexico, USA, p. 73. Portland, OR.
- Nayak, R., Stewart, T., Wang, R.-F., Lin, J., Cerniglia, C.E., Kenney, P.B., 2004. Genetic diversity and virulence gene determinants of antibiotic-resistant *Salmonella* isolated from preharvest turkey production sources. *Int. J. Food Microbiol.* 91, 51–62.
- NCCLS, 1993. Performance standards for antimicrobial disk susceptibility tests; Approved standard. NCCLS document M2-A5, NCCLS, 940 West Valley Road, Suite 1400, Wayne, PA 19087-1898, USA.
- NCCLS, 1998. Methods for dilution antimicrobial susceptibility tests for bacteria that grow aerobically—Fourth edition. NCCLS document M7-A4, NCCLS, 940 West Valley Road, Suite 1400, Wayne, PA 19087-1898, USA.
- Orr, K., Gould, F.K., Sisson, P.R., Lightfoot, N.F., Freeman, R., Burdess, D., 1991. Rapid inter-strain comparison by pyrolysis

- mass spectrometry in nosocomial infection with *Xanthomonas maltophilia*. J. Hosp. Infect. 17, 187–195.
- Radcliffe, C.E., Drucker, D.B., Boote, V., Fletcher-Williams, G., Claydon, M.A., 2001. Phospholipid analogue profiles of *Peptostreptococcus*, *Micromonas*, and *Finnegoldia* species analysed by fast atom bombardment mass spectrometry. Can. J. Microbiol. 47, 96–101.
- Rumelhart, D.E., McClelland, T.L., 1986. Parallel Distributed Processing. Bradford Books/MIT Press, Cambridge, MA.
- Sadek, F., Drucker, D.B., Boote, V., Bennett, K.W., Eley, A., 1998. Phospholipids of *Fusobacterium* spp. J. Appl. Microbiol. 85, 302–308.
- Salyers, A.A., 2002. An overview of the genetic basis of antibiotic resistance in bacteria and its implications for agriculture. Anim. Biotechnol. 13, 1–5.
- Salyers, A.A., Amabile-Cuevas, C.F., 1997. Why are antibiotic resistance genes so resistant to elimination? Antimicrob. Agents Chemother. 41, 2321–2325.
- Shen, H., Carter, J.F., Brereton, R.G., Eckers, C., 2003. Discrimination between tablet production methods using pyrolysis-gas chromatography-mass spectrometry and pattern recognition. Analyst 128, 287–292.
- Sisson, P.R., Freeman, R., Gould, F.K., Lightfoot, N.F., 1991a. Strain differentiation of nosocomial isolates of *Pseudomonas aeruginosa* by pyrolysis mass spectrometry. J. Hosp. Infect. 19, 137–140.
- Sisson, P.R., Freeman, R., Lightfoot, N.F., Richardson, I.R., 1991b. Incrimination of an environmental source of a case of Legionnaires' disease by pyrolysis mass spectrometry. Epidemiol. Infect. 107, 127–132.
- Sisson, P.R., Freeman, R., Magee, J.G., Lightfoot, N.F., 1991c. Differentiation between mycobacteria of the *Mycobacterium tuberculosis* complex by pyrolysis mass spectrometry. Tubercle 72, 206–209.
- Sisson, P.R., Freeman, R., Magee, J.G., Lightfoot, N.F., 1992a. Rapid differentiation of *Mycobacterium xenopi* from mycobacteria of the *Mycobacterium avium-intracellulare* complex by pyrolysis mass spectrometry. J. Clin. Pathol. 45, 355–357.
- Sisson, P.R., Kramer, J.M., Brett, M.M., Freeman, R., Gilbert, R.J., Lightfoot, N.F., 1992b. Application of pyrolysis mass spectrometry to the investigation of outbreaks of food poisoning and non-gastrointestinal infection associated with *Bacillus* species and *Clostridium perfringens*. Int. J. Food Microbiol. 17, 57–66.
- Smole, S.C., King, L.A., Leopold, P.E., Arbeit, R.D., 2002. Sample preparation of Gram-positive bacteria for identification by matrix-assisted laser desorption/ionization time-of-flight. J. Microbiol. Methods 48, 107–115.
- Snyder, J.W., 2003. Role of the hospital-based microbiology laboratory in preparation for and response to a bioterrorism event. J. Clin. Microbiol. 41, 1–4.
- Spining, M.T., Darsey, J.A., Sumpter, B.G., Noid, D.W., 1994. Opening up the black box of artificial neural networks. J. Chem. Educ. 71, 406–411.
- Török, T.J., Tauxe, R.V., Wise, R.P., Livengood, J.R., Sokolow, R., Mauvais, S., Birkness, K.A., Skeels, M.R., Horan, J.M., Foster, L.R., 1997. A large community outbreak of *salmonellosis* caused by intentional contamination of restaurant salad bars. J. Am. Med. Assoc. 278, 389–395.
- van Baar, B.L.M., 2000. Characterisation of bacteria by matrix-assisted laser desorption/ionization and electrospray mass spectrometry. FEMS Microbiol. Rev. 24, 193–219.
- Wilkes, J., Rafii, F., Glover, K., Holcomb, M., Cao, X., Sutherland, J., 2001. Microbial Identification Databases. US Patent Application No. 09/975,530, filed October 10, 2001.
- Wilkes, J.G., Glover, K.L., Holcomb, M., Rafii, F., Cao, X., Sutherland, J.B., McCarthy, S.A., Letarte, S., Bertrand, M.J., 2002. Defining and using microbial spectral databases. J. Am. Soc. Mass Spectrom. 13, 875–887.
- Willett, H.P., 1988. Antimicrobial agents. In: Joklik, W.K., Willett, H.P., Amos, D.B., Wilfert, C.M. (Eds.), Zinsser Microbiology, 19th ed. Appleton & Lange, Norwalk, CT, pp. 128–160.